AUT Journal of Mechanical Engineering

AUT J. Mech. Eng., 6(2) (2022) 179-188
DOI: 10.22060/ajme.2022.20391.5999

Comprehensive Evaluation of Human Hand Manipulability During Walking at Different Speeds

B. Miripour Fard[1]*, S. M. Bruijn[2], A. Hajiloo[3]

[1] Faculty of Mechanical Engineering, University of Guilan, Rasht, Iran
[2] Department of Human Movement Sciences, VU University, Amsterdam, Netherlands
[3] Independent Scholar, Los Angeles, California, USA

ABSTRACT: Using the experimental kinematic data of 11 healthy subjects, the kinematic manipulability of human hands during walking is evaluated. A total of 37 degrees of freedom mechanical model of the human body is used for this purpose. The forward kinematics and Jacobian of the model have been derived using the Denavit-Hartenberg convention. Experimental kinematics are mapped on the model using the inverse kinematic method based on optimization. The effect of walking speed on the profile and symmetry of manipulability for both right and left hands are studied. Statistical analysis showed that the walking speed can change the manipulability of hands and there is no quantitative symmetry between the manipulability of right and left hands. The results showed that there is more ability to create velocity for the hands-on horizontal plane than on other anatomical planes during walking. The results of sensitivity analysis showed the importance of the values of the hip and shoulder joints on the manipulability of the hands. The experimental manipulability profile of healthy human hands presented in this article can be used as a reference in rehabilitation to evaluate the effectiveness of physiotherapy as well as evaluation of hand function after surgery and also designing realistic motions for humanoids.

Review History:

Received: Aug. 11, 2021
Revised: Mar. 18, 2022
Accepted: Apr. 04, 2022
Available Online: Apr. 09, 2022

Keywords:

Hand movements
Manipulability
Kinematic mapping
Motion analysis

1- Introduction

The concept of manipulability was first introduced in robotics by Yoshikawa [1] for industrial robots. Manipulability is an indicator that each specific pose of the robot, determines the capacity to create speed in the end-effector of the robot in different directions. This criterion, defined by the robot Jacobian, is usually represented by an ellipse. The center of the ellipse is a point of the end-effector, and the capacity to create velocities in the direction of the elliptical diameters will vary. The volume of this ellipse will indicate the degree of total manipulation in a given posture. If the volume of the ellipse is zero, the robot will be in a singular position, and if the diameters of the ellipse are the same (sphere), the manipulability will be the same in all directions. There are many studies in the field of robotics on manipulability. In Ref. [2] a manipulability optimization control of a 7- Degree of Freedom (DoF) robot manipulator for Robot-Assisted Minimally Invasive Surgery (RAMIS) has been proposed. The relation between coordinates and manipulability analysis has been investigated in Ref. [3]. In this study, the dependency of manipulability on joint coordinates through the use of an appropriate metric has been removed. In Ref. [4] a distributed manipulability optimization scheme has been proposed to maximize the manipulability of redundant robot manipulators in a distributed network with limited communication. The concepts of manipulability measure and task compatibility are also extended to the free-floating closed chain system in Ref. [5]. In the field of humanoid robots, relatively little research has been done on manipulability. In most of these studies, the coordination of hands in performing tasks in a standing phase has been studied [6-10]. For example, in Ref. [6], the coordination of the fingers in performing tactile tasks on the phone has been investigated using the concept of manipulability. Also, in Ref. [7], the ability of the hands to grasp objects has been investigated using manipulability. Some studies have also studied the hand manipulation of the humanoid robot as it moves [8-11]. In Ref. [12] single and dual-arm manipulability of human movements during the execution of industry-like activities has been studied. Manipulability has also been used for optimizing human working configuration [13].

In robotic research on manipulability, there are interesting results about the human body, for example, it has been found that approximately equal arm and forearm length in the human hand maximizes hand manipulability. Humans also subconsciously place their elbows at a 90-degree angle when writing. It can easily be shown that in this posture the manipulability is maximized [14].

The human body can be modeled like manipulators. A tree structure can be considered for modeling, each branch of which consists of a serial arm. With such modeling, the concept of manipulability for the human model can also be

*Corresponding author's email: bmf@guilan.ac.ir

evaluated.

In Refs. [15] and [16], swing foot manipulability during walking has been studied and its relationship with stability and selection of motor strategies has been investigated. The results showed that swing foot manipulability can explain the reason for choosing movement strategies during perturbed walking. Also, in these studies, the manner of changes in the manipulability of the swing foot in the single support phase has been determined. The results showed that manipulability can affect the step size and consequently the stability.

In continuation of our previous research, in the present work, the aim is to conduct a comprehensive and experimental study to investigate the manipulability of the human hands while walking, to use it in rehabilitation as well as designing and path planning of humanoid robots. Having a comprehensive reference to the normal profile of the manipulability changes of a healthy human hand during walking can be used to design exoskeletons [17, 18], and to assess the improvement of injured people during rehabilitation treatment. It will also be possible to imitate these profiles to create natural movements for digital human models and humanoid robots. Moreover, not considering this index in the ergonomic design of objects such as backpacks and walking assistance devices and training systems can reduce the human ability to grasp and reach objects around in order to maintain stability and avoid falling.

To our best knowledge, there is no previous research in the literature that experimentally analyzes the manipulability of arms during human walking. The novelty of current work is to address this issue and to answer the following questions: (1) How does the manipulability of human hands change when walking? (2) Can walking speed affect hand manipulability? (3) Is there symmetry between left- and right-hand manipulability when walking? (4) Angle changes in which joints have the greatest impact on the kinematic manipulability of hands?

The rest of this article is organized as follows: The methods used in the current paper for modeling, performing experiments, and mapping experimental data to the model are introduced in section 2. Section 3 shows the results and discussion. Finally, concluding remarks are given in section 4.

2- Method

This section explains the modeling of the human body and the calculation of hand manipulability. It also describes how to map experimental kinematic data to the model.

2- 1- Modeling and calculating manipulability

A dynamical model of the human body that we have developed in the previous works [15, 16] has been used in this research. The model and coordinates assigned based on the Denavit-Hartenberg convention [19] are shown in Fig. 1.

The model has 31 revolute joints and the total degrees of freedom of the model is 37 (considering the 6 degrees of freedom for the stance foot in 3D space). The structure of the model can be considered as a tree [8]. For example, in the single support phase, where the right foot is the support, the right leg is considered as the trunk, and the left foot and two hands can be considered as branches. In other words, in this case, there are three manipulators, and the corresponding end-effectors are the tip of the swing foot (left foot), left and right hands. For each of these branches, the corresponding Jacobian and consequently manipulability can be defined independently.

The relationship between joint velocities and end-effector velocities can be expressed as follows:

$$\begin{pmatrix} \xi_{\mathbf{L}} \\ \xi_{\mathbf{R}} \end{pmatrix} = \mathbf{J} \begin{pmatrix} \dot{q}_1 \\ \vdots \\ \dot{q}_{31} \end{pmatrix}, \quad \mathbf{J} = \begin{pmatrix} \mathbf{J}_{\mathbf{L}}^{\mathbf{1}} & \mathbf{J}_{\mathbf{L}}^{\mathbf{2}} \\ \mathbf{J}_{\mathbf{R}}^{\mathbf{1}} & \mathbf{J}_{\mathbf{R}}^{\mathbf{2}} \end{pmatrix} \tag{1}$$

In Eq. (1) $\xi_{\mathbf{L}}$ and $\xi_{\mathbf{R}}$ are 6×1 vectors that show the linear velocities and the angles of the left and right ends of the hand, respectively. $\dot{q}_i$ represents the velocity of the angles of the i-th joint. $\mathbf{J}$ denotes the Jacobian matrix. Each element of $\mathbf{J}$ (i.e., $\mathbf{J}_{\mathbf{L}}^{\mathbf{1}}, \mathbf{J}_{\mathbf{L}}^{\mathbf{2}}$, $\mathbf{J}_{\mathbf{R}}^{\mathbf{1}}$ and $\mathbf{J}_{\mathbf{R}}^{\mathbf{2}}$) is a 6×m matrix that represents the Jacobian of the joints that affects the velocity of the corresponding hand. Subscripts R and L stand for right and left respectively. It should be noted that the movement of the joints of the left hand has no effect on the speed of the end of the right hand and vice versa. Also, the movements of the joints of the swing foot branch do not have a direct effect on the velocity of the hands. Eq. (1) can also be written compactly $\xi = \mathbf{J}(\mathbf{q})\dot{\mathbf{q}}$ (see Appendix). Accordingly, manipulability is defined as follows [1]:

$$w = \sqrt{\det(\mathbf{J}(q)\mathbf{J}^{\mathrm{T}}(q))} \tag{2}$$

According to Eq. (2), manipulability is directly dependent on the Jacobian. If the model is in a singular state, the amount of manipulability is zero, which means an inability to move in different directions.

To evaluate the ability of the model to create velocity in different directions, the manipulability ellipse is plotted. To do so, it is assumed that an angular velocity with the unit norm is imposed on the joints of the model. The equation of ellipsoid can be written as follows [19]:

$$\xi^{\mathrm{T}}[\mathbf{J}(q)\mathbf{J}^{\mathrm{T}}(q)]^{-1}\xi = 1 \tag{3}$$

In manipulability analysis, the volume and shape of the ellipsoid are very important. If this ellipse becomes a sphere, it indicates that the capacity to create velocity is the same in all directions. Otherwise, it will be able to accelerate in the

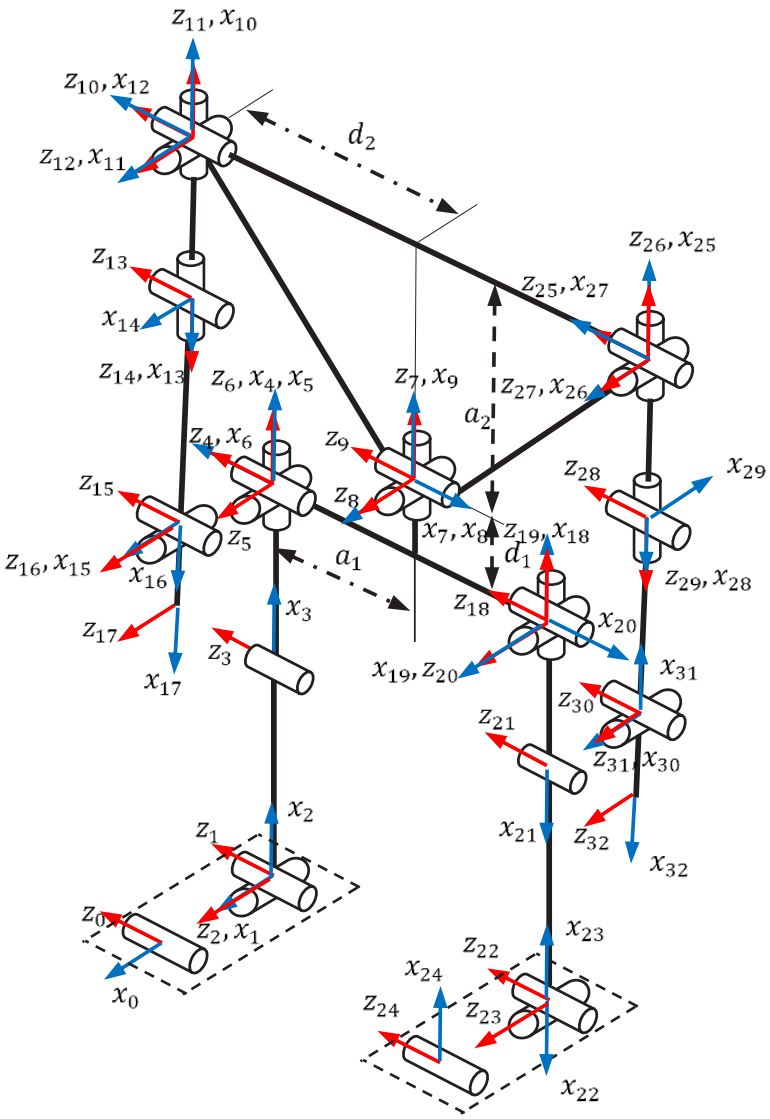

Fig. 1. The dynamic model of the human body and assigned coordinates

direction of the major axis. In other words, the manipulability in this direction will be more. The volume of this ellipse represents the total size of the manipulability (w) given in Eq. (2).

2- 2- Experimental motion analysis data and mapping on the model

Raw experimental data from the motion analysis system recorded at Vrije Universiteit in Amsterdam are used in this paper [20]. These data provide the coordinates of markers on the body of 11 subjects while walking on a treadmill at different speeds. The general anthropometric parameters of the subjects are given in Table 1.

The experiment protocol has been approved by the Ethics Committee of the Vrije Universiteit and all subjects signed the consent forms for the trials. Each subject walked on a treadmill at three different speeds (0.56, 1.12, and 1.68) meters per second for 5 minutes. The motion analysis system recorded the position of 39 reflective markers on the subject's body at a frequency of 50 Hz.

2- 3- Mapping experimental data on the model

Manipulability is not a quantity that can be calculated directly for each subject. It is necessary to map the kinematics of each subject's motion on the corresponding model and then calculate the manipulability by knowing the Jacobian equations of the model. One method for mapping experimental data is to consider virtual markers on the model, and then obtain the values of the joint angles of the model in such a way that the difference between the position of virtual and real markers is zero or minimal. This method leads to the formation of an optimization problem in which the objective

Table 1. Anthropometric parameters of 11 healthy male subjects example of a table

Parameter	Mean	Standard Deviation
Age (Year)	27.7	3.3
Height (m)	1.80	0.06
Weight (kg)	75.50	0.90

function is defined as follows:

$$\text{cost} = \min_{\mathbf{q}} \sum_{i=1}^{n} w_i \left\| x_i^{\exp} - x_i^{v}(\mathbf{q}) \right\|^2 \quad (4)$$

In Eq. (4), $x_i^{\exp}$ is the real physical marker position obtained from experiments on subjects and x_i^{v} is the virtual marker position. w_i is the weight factor that is considered depending on the importance of each joint. By solving this optimization problem for each sample time of the walk, a vector of joint angles for the model is obtained which corresponds to the real posture of the subject. To solve the optimization problem, a hybrid genetic algorithm method has been used. The optimization problem is solved in MATLAB software. For more information on the method, as well as the optimization constraints and the assumed weight coefficients, see the Appendix section.

3- Results and Discussion

The evolution of the manipulability index of the left and right hands during walking at different speeds is shown in Fig. 2. From Fig. 2a, it is evident that if the left foot is in the stance phase (support phase), the left-hand manipulability index does not change much during the swinging of the other foot. A similar result can be stated for the right foot (Fig. 2d). According to the results of Figs. 2a and 2d, it can be concluded that the manipulation of the right hand is slightly higher than the left hand. However, if the left foot is supported, the manipulability of the right hand is less than the manipulability of the left hand when the right foot is supported (Figs. 2b and 2c)

It is worth noting that a difference between the manipulability of the right and left hands is seen in Fig. 2. Previous research has shown that the kinematic asymmetry of arm-swing is not related to handedness [21]. Therefore, given that the manipulability is calculated based on kinematics, the observed difference between the manipulability results between the right and left hands (Fig. 2) is not related to handedness.

To identify regionally specific effects of walking speed on manipulability, one-dimensional Statistical Parametric Mapping (SPM1D) repeated measures ANOVA has been used. SPM1D is a package for one-dimensional Statistical Parametric Mapping [22, 23]. It uses random field theory to make statistical inferences regarding registered (normalized) sets of 1D measurements. The results of SPM1D repeated measures ANOVA for hands are depicted in Fig. 3. Both the manipulability of left and right hands showed increases in manipulability with increasing walking speed, although only in certain parts of the gait cycle (see Figs. 2 and 3).

The hand manipulability ellipsoids are shown in Figs. 4 to 6 at the early-, mid-and late-swing phases of walking from three different views. It is clear from Fig4 . that the major and minor axes of the ellipses for the right and left hands are different, but the volume of the ellipses is almost the same. At the mid-swing phase (Fig. 5) and on the sagittal plane, the axes of the ellipses are approximately parallel. Also, in this phase, as in the previous phase, the volumes of the hand's manipulability ellipsoids are almost the same. In the late-swing phase (Fig. 6), the axes of the ellipses are not in the same direction for the right and left hand and the volume of the ellipses are different in sagittal and frontal planes. From Figs. 4 to 6 it is clear that the ability of both hands to create velocity in the horizontal plane is more than in the other two planes.

The manipulability index is defined based on the Jacobian and is related to the joint variables of the model/subject. A sensitivity analysis is conducted to investigate how the variation in the manipulability of the model can be attributed to variations of joint angles. The Elementary Effects (EEs) method [24] was used for the sensitivity analysis to identify important joint variables. The average Elementary Effects of the variation of joint angles on the manipulability against their standard deviations are depicted in Figs. 7 and 8 for the right swing hand and left swing hand, respectively.

The top three sensitive parameters for the left-hand manipulability index during the right stance phase are left shoulder abduction/adduction, left shoulder extension/ flexion, and left elbow flexion/extension (Fig. 7). For the right-hand manipulability during the right stance phase, the more important parameters are the right shoulder extension/ flexion, right shoulder abduction/adduction, and right hip flexion/ extension (Fig. 8). Similar results are obtained during the left foot stance phase.

(a) Manipulability of left hand, left stance phase

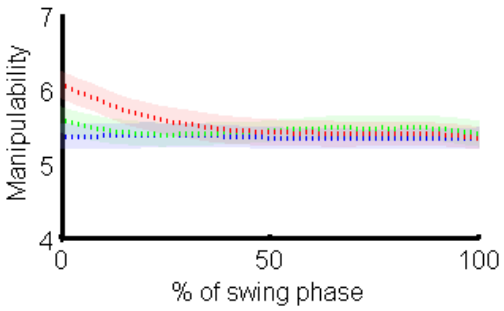

(b) Manipulability of right hand, left stance phase

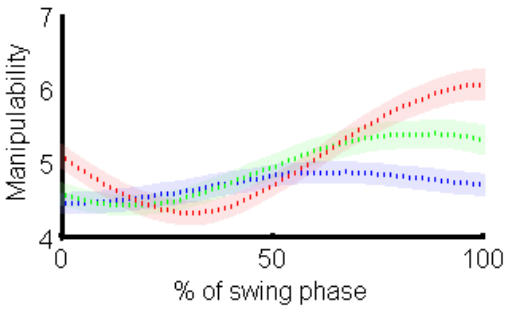

(c) Manipulability of left hand, right stance phase

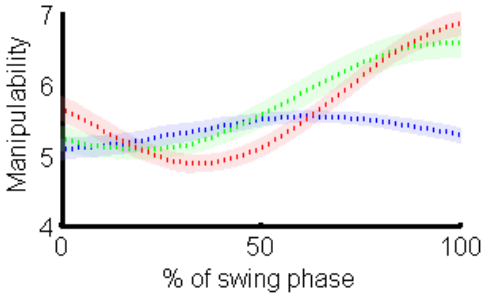

(d) Manipulability of right hand, right stance phase

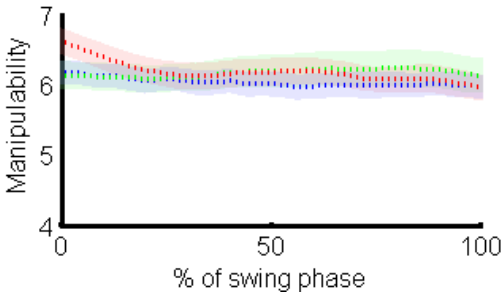

Fig. 2.Manipulability of the right and left swing hands for different speeds ($v_1 = 0.56\mathbf{ms}^{-1}$, $v_2 = 1.12\mathbf{ms}^{-1}$, $v_3 = 1.68\mathbf{ms}^{-1}$). Dashed lines show the mean (M) and shaded clouds (E) indicate the standard deviation envelope.

4- Conclusion

Experimental analysis of human hand manipulability was performed in this study. Profiles of changes in this index were provided during walking at different speeds. Both the manipulability of left and right hands showed increases in manipulability with increasing walking speed. The results showed that there is more ability to create velocity for the hands-on horizontal plane than on other anatomical planes. Quantitatively, there is no symmetry between the left and right-hand manipulability, but the trend of changes in this index during walking is almost the same for both hands (Fig. 2). Sensitivity analysis showed that the hip and shoulder joints have a most important effect than other joints on the manipulability of the hands. Therefore, it is recommended to pay more attention to these joints in designing exoskeletons and ergonomic equipment. In the other words, considering the manipulability of hands in the ergonomic design of equipment ensure that human users are enabled to function properly and dexterously. The experimental manipulability profile of healthy human hands presented in this article can be used as a reference in rehabilitation to evaluate the effectiveness of physiotherapy as well as evaluation of hand function after surgery. The result can also be used in the path planning of humanoid robot hands.

Appendix

Jacobian matrix

The Jacobean is calculated only for the swing phase of walking. The model has three serial sub-structures with three end-effectors. So, the body velocity in the right hand of the (1) is a $6N \times 1$ vector (N=3), and the Jacobian matrix is a $6N \times 31$ matrix (N=3)

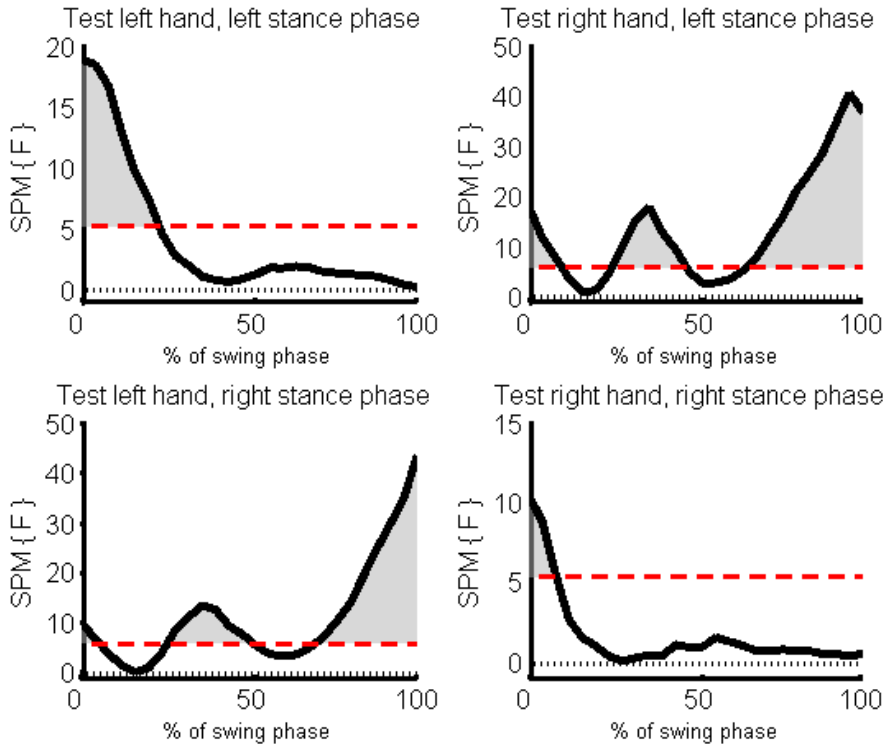

Fig. 3. SPM1D repeated measures ANOVA of right and left swing hands for manipulability index. Three walking speeds were considered. F* (red dashed line) is the significance level of SPM.

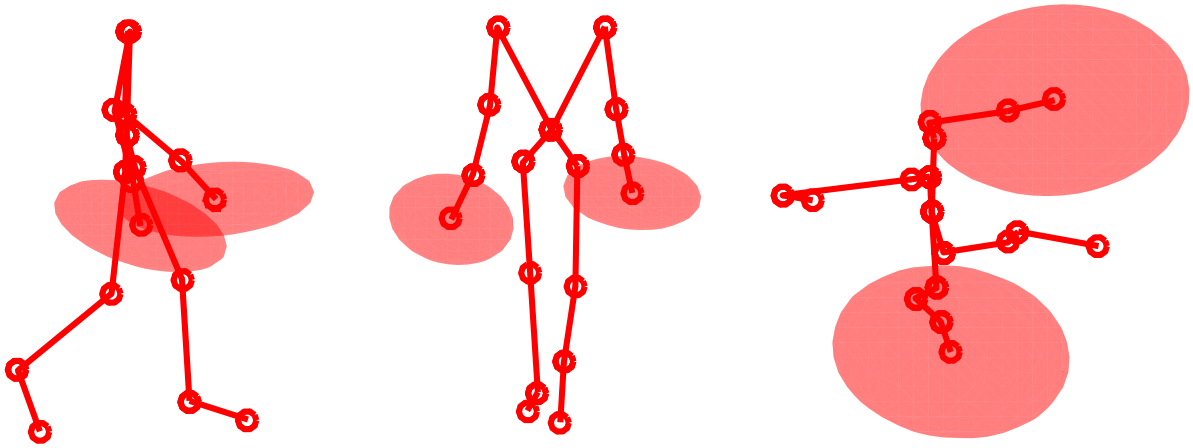

Sagittal view Frontal view Horizontal view

Fig. 4. Manipulability ellipsoids for the hands in the early-swing phase. The right foot is the support.

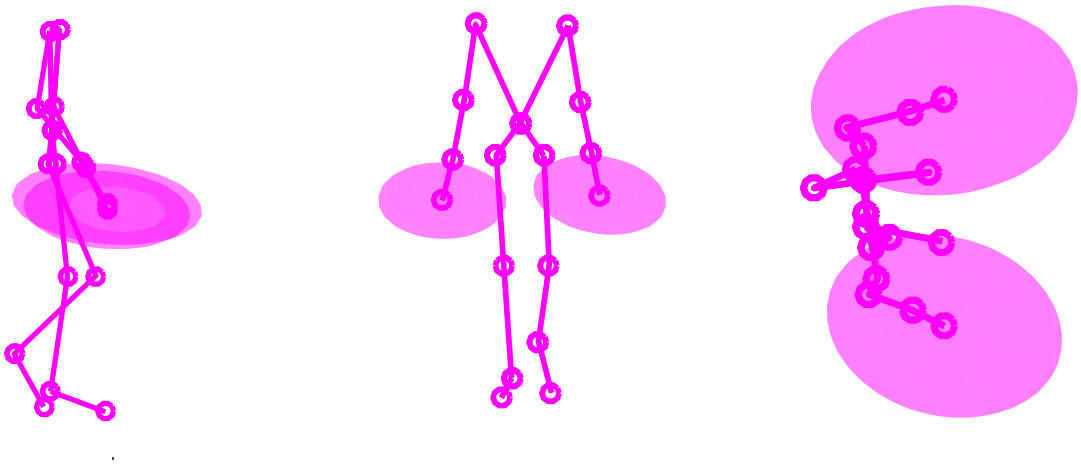

Fig. 5. Manipulability ellipsoids for the hands in the mid-swing phase. The right foot is the support.

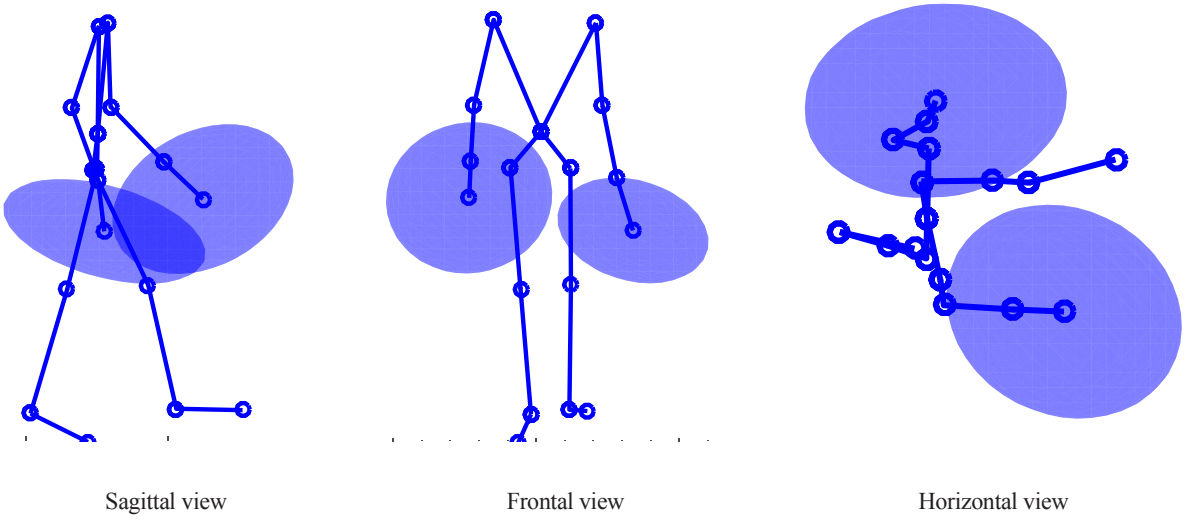

Fig. 6. Manipulability ellipsoids for the hands in the late swing phase. The right foot is the support.

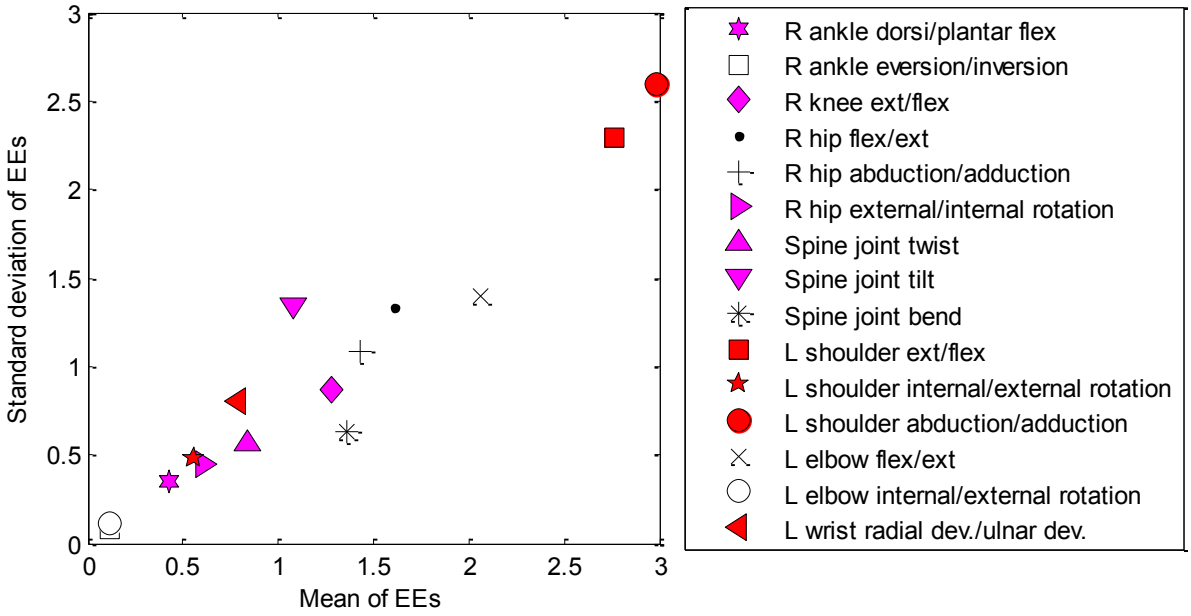

Fig. 7. Mean of Elementary Effects (EEs) and standard deviation for left swing hand. The legend is abbreviated. L stands for left, R stands for Right, flex stands for flexion and ext stands for the extension.

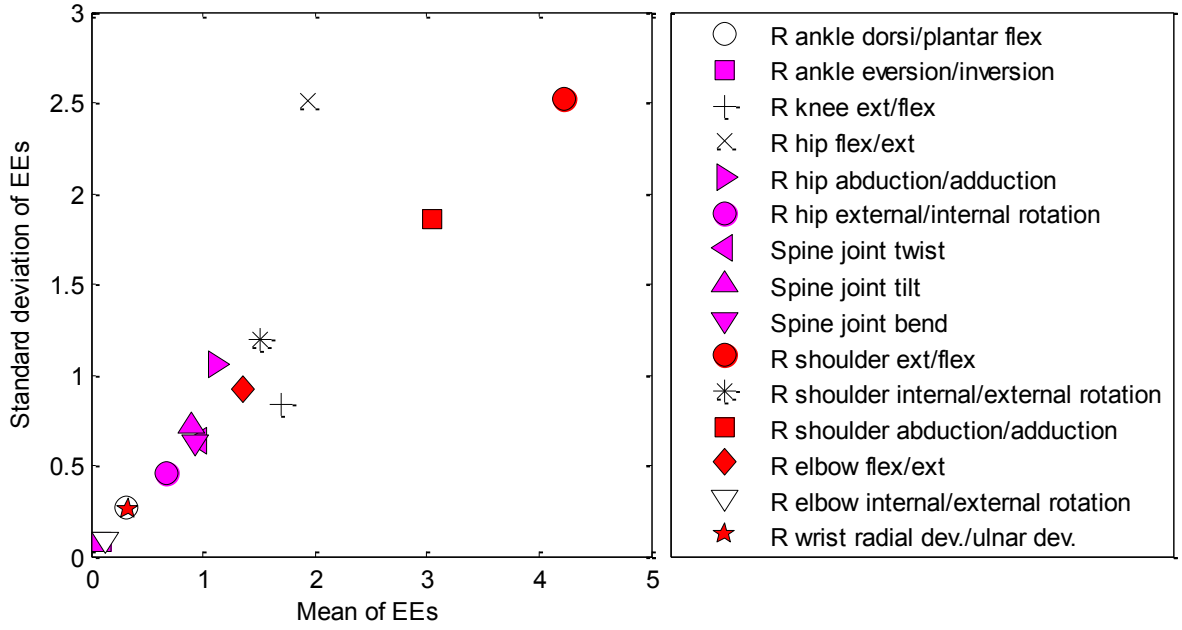

Fig. 8. Mean of Elementary Effects (EEs) and standard deviation for right swing hand. The legend is abbreviated. L stands for left, R stands for Right, ex stands for extension and flex stands for flexion.

Table 2. Value of the weights (w_i) used in the optimization cost.

Marker Name	Weight	Marker Name	Weight	Marker Name	Weight
Right toe	1	Right ankle	10	Right knee	10
Left toe	1	Left ankle	10	Left knee	10
Right hip	10	Right wrist	5	Right shoulder	10
Left hip	10	Left wrist	5	Left shoulder	10
Right elbow	20	Right hand	30	pelvis	10
Left elbow	20	Left hand	30		

$$\begin{pmatrix} \xi_1 \\ \xi_2 \\ \xi_3 \end{pmatrix} = \begin{pmatrix} \mathbf{J}_1^1 & \mathbf{J}_1^2 & \mathbf{J}_1^3 \\ \mathbf{J}_2^1 & \mathbf{J}_2^2 & \mathbf{J}_2^3 \\ \mathbf{J}_3^1 & \mathbf{J}_3^2 & \mathbf{J}_3^3 \end{pmatrix} \begin{pmatrix} \dot{q}_1 \\ \vdots \\ \dot{q}_{31} \end{pmatrix}$$

in which ξ_i (i=1..3) is a 6×1 vector containing the linear and angular velocities of the end-effector i. $\mathbf{J}_i^j$ is a 6×m matrix where the m depends on the number of the joints that influence the velocity of the corresponding end-effector.

Constraints and weight matrix of the optimization problem

Table 2. shows the weights used in the optimization cost (Eq. (4)).

The joint angles (***q***) are the design variables of the optimization in each frame of motion. The cost function (Eq. (4)) is subject to the constraints on physiological limitation of joint angles. The lower and upper bounds on the design variables (in radians) are considered as follows, respectively:

lb=[-60,60,0,0,-30,40,160,-30,70,-70,-130,-120,-10,90,-50,-110,-30,120,60,-120,-90,-200,0,150,-110,50,-90,150,50,150]*π/180;

ub=[60,150,10,60,90,120,210,30,120,20,30,-60,120,180,50,-70,30,-30,120,-60,0,-160,10,0,-70,180,60,210,130,210]*π/180;

Optimization method

A hybrid scheme is used to optimize the cost function (Eq. (4)) using the Genetic Algorithm (GA) and fmincon which is a gradient-based method. GA can quickly reach a neighborhood of a local minimum, but it can require many function evaluations to achieve convergence. In the hybrid approach, first GA is used to approach a point near the optimum point. In this stage, a small number of generations is used to speed the solution process. Then, the solution from GA is used as the initial point for the fmincon solver to perform a faster and more efficient local search.

References

[1] T. Yoshikawa, Manipulability of robotic mechanisms, The international journal of Robotics Research, 4(2) (1985) 3-9.

[2] H. Su, S. Li, J. Manivannan, L. Bascetta, G. Ferrigno, E. De Momi, Manipulability optimization control of a serial redundant robot for robot-assisted minimally invasive surgery, in: 2019 International Conference on Robotics and Automation (ICRA), IEEE, 2019, pp. 1323-1328.

[3] J. Lachner, V. Schettino, F. Allmendinger, M.D. Fiore, F. Ficuciello, B. Siciliano, S. Stramigioli, The influence of coordinates in robotic manipulability analysis, Mechanism and machine theory, 146 (2020) 103722.

[4] J.Z. L. Jin, X. Luo,M. Liu,Sh. Li, L. Xiao,Z. Yang, Perturbed Manipulability Optimization in a Distributed Network of Redundant Robots, IEEE Transactions on Industrial Electronics, 68(8) (2021) 7209-7220.

[5] J.L. Ruonan Xu, Mingming Wang, Kinematic and dynamic manipulability analysis for free-floating space robots with closed chain constraints, Robotics and Autonomous Systems, 130 (2020) 1035-1049.

[6] H. Endo, Application of robotic manipulability indices to evaluate thumb performance during smartphone touch operations, Ergonomics, 58(5) (2015) 736-747.

[7] N. Vahrenkamp, T. Asfour, G. Metta, G. Sandini, R. Dillmann, Manipulability analysis, in: 2012 12th ieee-ras international conference on humanoid robots (humanoids 2012), IEEE, 2012, pp. 568-573.

[8] J. Jacquier-Bret, P. Gorce, N. Rezzoug, The manipulability: a new index for quantifying movement capacities of upper extremity, Ergonomics, 55(1) (2012) 69-77.

[9] I. Lee, J.-H. Oh, Humanoid posture selection for reaching motion and a cooperative balancing controller, Journal of Intelligent & Robotic Systems, 81(3-4) (2016) 301-316.

[10] J. Lenarcic, N. Klopcar, Positional kinematics of humanoid arms, Robotica, 24(1) (2006) 105.

[11] K. Inoue, H. Yoshida, T. Arai, Y. Mae, Mobile manipulation of humanoids-real-time control based on manipulability and stability, in: Proceedings 2000 ICRA. Millennium Conference. IEEE International Conference on Robotics and Automation. Symposia Proceedings (Cat. No. 00CH37065), IEEE, 2000, pp. 2217-2222.

[12] N. Jaquier, L. Rozo, S. Calinon, Analysis and Transfer of Human Movement Manipulability in Industry-like Activities, arXiv preprint arXiv:2008.01402, (2020).

[13] L. Peternel, D.T. Schøn, C. Fang, Binary and Hybrid Work-Condition Maps for Interactive Exploration of Ergonomic Human Arm Postures, Frontiers in Neurorobotics, 14 (2021) 114.

[14] T. Yoshikawa, Foundations of robotics: analysis and control, MIT press, 1990.

[15] B.M. Fard, A manipulability analysis of human walking, Journal of biomechanics, 83 (2019) 157-164.

[16] B.M. Fard, S.M. Bruijn, On the manipulability of swing foot and stability of human locomotion, Multibody System Dynamics, 46(2) (2019) 109-125.

[17] T. Petrič, L. Peternel, J. Morimoto, J. Babič, Assistive arm-exoskeleton control based on human muscular manipulability, Frontiers in neurorobotics, 13 (2019) 30.

[18] Y. Wang, J. Qiu, H. Cheng, X. Zheng, Analysis of Human–Exoskeleton System Interaction for Ergonomic Design, Human factors, (2020) 0018720820913789.

[19] M.W. Spong, S. Hutchinson, M. Vidyasagar, Robot modeling and control, John Wiley & Sons, 2020.

[20] S.M. Bruijn, O.G. Meijer, P.J. Beek, J.H. van Dieën, The effects of arm swing on human gait stability, Journal of experimental biology, 213(23) (2010) 3945-3952.

[21] J. Kuhtz-Buschbeck, K. Brockmann, R. Gilster, A. Koch, H. Stolze, Asymmetry of arm-swing not related to handedness, Gait & posture, 27(3) (2008) 447-454.

[22] T.C. Pataky, Generalized n-dimensional biomechanical field analysis using statistical parametric mapping, Journal of biomechanics, 43(10) (2010) 1976-1982.

[23] T.C. Pataky, J. Vanrenterghem, M.A. Robinson, Zero- vs. one-dimensional, parametric vs. non-parametric, and confidence interval vs. hypothesis testing procedures in one-dimensional biomechanical trajectory analysis, Journal of biomechanics, 48(7) (2015) 1277-1285.

[24] F. Pianosi, F. Sarrazin, T. Wagener, A Matlab toolbox for global sensitivity analysis, Environmental Modelling & Software, 70 (2015) 80-85.

HOW TO CITE THIS ARTICLE

B. Miripour Fard, S. M. Bruijn, A. Hajiloo, Comprehensive Evaluation of Human Hand Manipulability During Walking at Different Speeds, AUT J. Mech Eng., 6(2) (2022) 179-188.

DOI: 10.22060/ajme.2022.20391.5999